Roman Core Community Surveys White Paper: Coordinating Roman and Rubin for Cosmic Probes of Dark Matter with Resolved Stellar Populations

Roman Core Community Survey: High Latitude Wide Area Survey

Scientific Categories: stellar populations and the interstellar medium, galaxies, large scale structure of the universe

Additional scientific keywords: Galaxies: Galaxy dark matter halos, Stellar Populations (and the ISM): Dwarf galaxies, Large Scale Structure of the Universe: Dark matter distribution

Submitting Author:
Name: Keith Bechtol
Affiliation: University of Wisconsin-Madison
Email: kbechtol@wisc.edu

List of contributing authors (including affiliation and email):

- Kabelo Tsiane, University of Chicago, kabelo@uchicago.edu
- Alex Drlica-Wagner, Fermilab, kadrlica@fnal.gov
- Peter Ferguson, University of Wisconsin-Madison, peter.ferguson@wisc.edu
- Sebastian Banaszak, University of Wisconsin-Madison, smbanaszak@wisc.edu
- Christian Aganze, University of California San Diego, caganze@ucsd.edu
- Sarah Pearson, New York University, spearson@nyu.edu
- Tjitske Starkenburg, Northwestern University, tjitske.starkenburg@northwestern.edu
- Ethan O. Nadler, Carnegie Observatories & University of Southern California, enadler@carnegiescience.edu
- Nushkia Chamba, The Oskar Klein Centre/Stockholm University, nushkia.chamba@astro.su.se
- Sidney Mau, Stanford University, smau@stanford.edu
- Jeffrey L. Carlin, Vera C. Rubin Observatory/AURA, jcarlin@lsst.org
- Nora Shipp, Massachusetts Institute of Technology, nshipp@mit.edu
- Risa Wechsler, Stanford University & SLAC National Accelerator Laboratory, rwechsler@stanford.edu

Abstract

We advocate for coordinated survey design between the Nancy Grace Roman Space Telescope and Vera C. Rubin Observatory to enhance cosmic probes of dark matter, in particular, by using combined observations and analysis of resolved stellar populations throughout the Local Volume. Using a joint simulation of the Rubin Observatory Legacy Survey of Space and Time (LSST) and Roman High Latitude Wide Area Survey (HLWAS), we show that the discovery and characterization of ultra-faint galaxies and stellar streams with ground-based imaging alone is likely to be limited by star-galaxy confusion and blending effects. An efficient way to overcome these challenges, and take advantage of the unprecedented capabilities of both facilities, would be to image a substantial fraction of the LSST Wide-Fast-Deep survey footprint with at least one band as a component of the Roman HLWAS. The combination of deep optical to near-IR multiband photometry and space-based angular resolution would yield a high-purity stellar sample of broad utility for Galactic studies and near-field cosmology that could not be obtained with either survey alone.

1 Cosmic Probes of Dark Matter

Astrophysical observations probe the physics of dark matter through its impact on structure formation throughout cosmic history. Fundamental properties of dark matter — e.g., particle mass, self-interaction cross section, coupling to the Standard Model, and non-standard time evolution such as dark matter decays — can imprint themselves on the macroscopic distribution of dark matter in a detectable manner by modifying the abundance, density profiles, and spatial distribution of dark matter halos. Astrophysical observations offer unique sensitivity to a wide range of dark matter particle models (including particle candidates that interact only through gravity) and are highly complementary to terrestrial experiments and indirect dark matter searches. Additionally, measurements of the dark matter distribution across a wide range of physical length scales can be used to constrain the physics of the early Universe, including inflation as well as non-standard cosmologies, e.g., with early matter domination.

In the coming years, Roman-Rubin coordination could advance multiple techniques to study dark matter halos near and below the minimum mass threshold to host stellar populations. These halos offer unique advantages to constrain the microphysical properties of dark matter because their evolution is less affected by complicated baryonic physics and because many "non-minimal" dark matter properties leave the most conspicuous signatures on low-mass halos. In this Roman Core Community Survey white paper, we highlight specific opportunities for Roman-Rubin coordination in the area of near-field cosmology with resolved stellar populations.

The combination of ground-based optical (Rubin) + space-based near-IR (Roman) imaging would provide accurate star–galaxy classification to enable detailed studies of the Milky Way stellar halo as well as ultra-faint galaxies and stellar streams up to several Mpc beyond the Milky Way virial radius, taking full advantage of the unprecedented depth of both surveys. We would be able to conduct a detailed census of the low-mass galaxies throughout the Local Volume to firmly establish the threshold halo mass for galaxy formation (likely $\sim 10^8$ solar masses), and search for density perturbations in stellar streams caused by interactions with even lower-mass dark matter halos (10^6 - 10^8 solar masses).

1.1 Ultra-faint Galaxies to the Milky Way Virial Radius and Beyond

Low mass and low stellar density ultra-faint galaxies trace the dark matter distribution on the smallest physical scales that have been explored to date, with demographic studies yielding competitive constraints on the fundamental nature of dark matter (e.g., Nadler et al., 2021). Such low luminosity galaxies are usually recognized in wide-field optical and near-IR imaging surveys as arcmin-scale statistical overdensities of *individually resolved member stars*. Accordingly, discovery and analysis of ultra-faint galaxies critically depends on having a high-purity and high-completeness stellar sample that extends to the faintest possible magnitudes. The deep imaging capabilities of Rubin and Roman will extend sensitivity to ultra-faint galaxies at distances of several Mpc that are only partially resolved in ground-based imaging data alone (Figure 1).

To forecast the potential gains of combining Roman and Rubin observations to study ultra-faint galaxies, we analyzed a joint simulated dataset of the same universe observed with Roman and Rubin (Troxel et al., 2023). First, we quantify the impact of star-galaxy confusion on searches for ultra-faint galaxies in LSST by injecting synthetic populations of member stars at the catalog level with realistic photometric measurement uncertainties, and test our ability to recover those synthetic ultra-faint galaxies. Figure 2 compares the sensitivity of LSST as a function of the luminosity, size, and

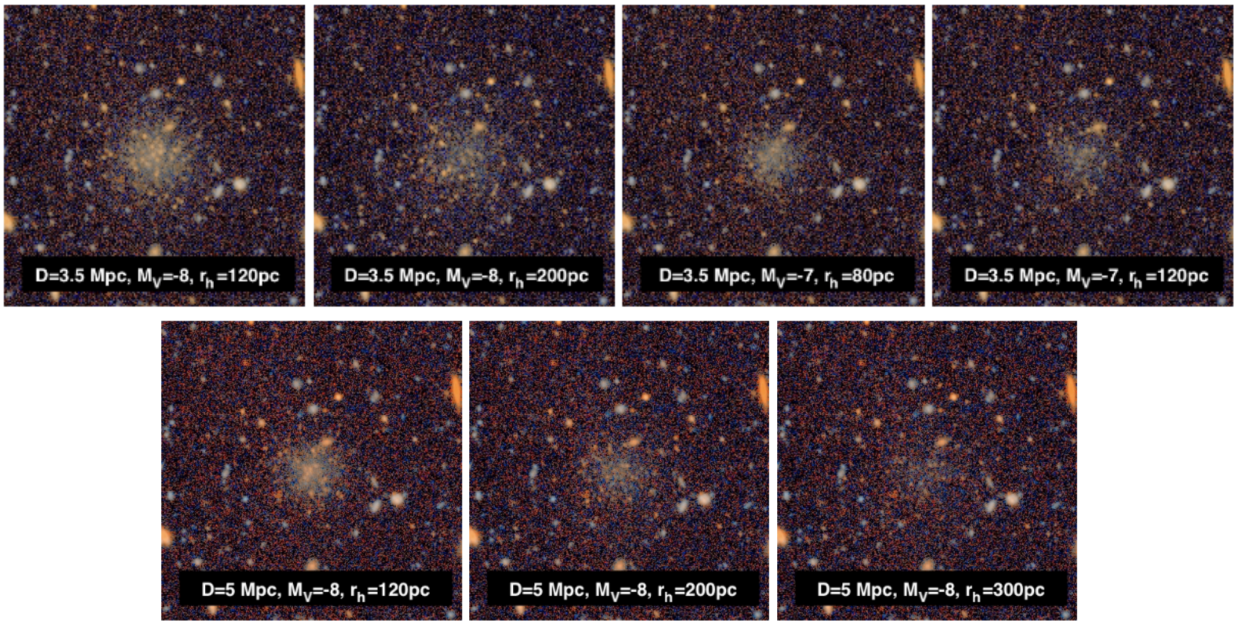

Figure 1: RGB false color images of example simulated faint dwarf galaxies as would be seen in Rubin Observatory/LSST. Each image cutout is $1\,\mathrm{arcmin} \times 1\,\mathrm{arcmin}$. The top row shows galaxies of varing size and luminsoity at a distance of 3.5 Mpc. The bottom row shows galaxies of increasing size at a distance of 5 Mpc. Detection and characterization of such galaxies using ground-based imaging alone will be limited by star-galaxy confusion and blending effects. Reproduced from Mutlu-Pakdil et al. (2021).

distance of ultra-faint galaxies *with* and *without* the effect of star-galaxy confusion. When considering realistic star-galaxy confusion in deep ground-based imaging data alone, we see that the discovery space for ultra-faint galaxies in the outer halo of the Milky Way and beyond is substantially limited compared to the case of ideal star-galaxy classification. **The sensitivity of Rubin/LSST alone to ultra-faint galaxies will be primarily limited by star-galaxy confusion rather than the raw imaging depth.**

Figure 3 shows the impact of star-galaxy for an example ultra-faint galaxy near the threshold of detection. With LSST alone, faint unresolved galaxies that are mistakenly classified as stars vastly outnumber the true stars in the field population, and thus present a dominant background to ultra-faint galaxy searches.

Next, we forecast improvements to star-galaxy classification accuracy that could be realized by joining LSST with space-based Roman imaging. The simulated Roman-Rubin dataset includes the Monte Carlo truth classification of every object rendered in the survey images, so we can directly evaluate the expected accuracy of star-galaxy classification for realistic measurements in both surveys. Figures 4 and 5 show that large numbers of faint unresolved galaxies contaminate the sample of classified stars from LSST fainter than $i \sim 24\,\mathrm{mag}$. **Combining LSST with a single band of Roman imaging could enable robust star/galaxy classification to the $SNR \sim 10$ imaging depth of LSST.**

The same considerations for star-galaxy classification apply for analyses of stellar streams around the Milky Way (as well as extragalactic stellar streams, discussed further in Section 1.2). Indeed, nearly all studies of faint resolved stellar populations in LSST would be enhanced with accurate star-galaxy

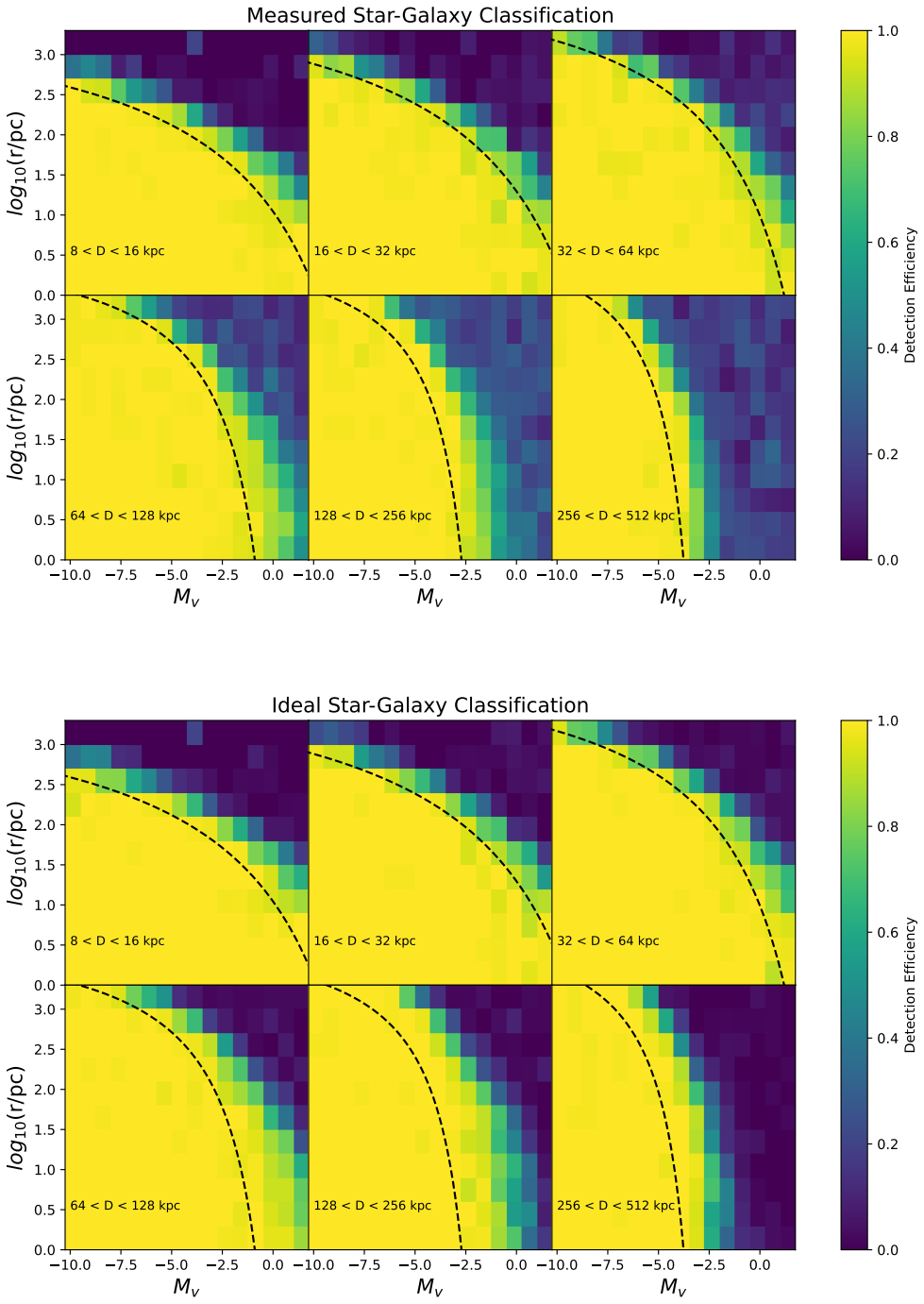

Figure 2: Forecasted detection efficiency for Milky Way satellite galaxies in LSST Year 5 imaging as a function of luminosity (M_V), physical size (r), and distance (D). The black dashed curves show contours of 50% detection efficiency in Dark Energy Survey (DES) Year 3 data. *Top*: Measured star-galaxy classification. *Bottom*: Ideal star-galaxy classification. **Inability to distinguish unresolved background galaxies from stars at the faint end limits LSST sensitivity to roughly comparable thresholds as DES, while the "ideal" case shows that there is much more discovery space with improvements in star-galaxy separation.**

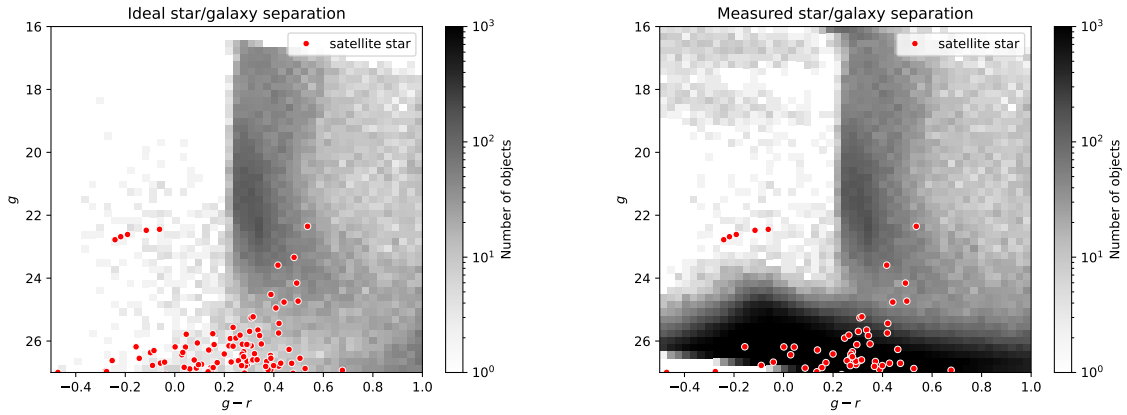

Figure 3: Simulated photometry of individually resolved member stars in a representative ultra-faint galaxy with luminosity $M_V \sim -2.5$ at a distance of 240 kpc as seen in the 5-year LSST data release (red points). The color-magnitude distribution of field population of objects classified as stars is shown in grayscale. *Left*: With ideal star/galaxy classification, the main sequence stars in the ultra-faint galaxy could be clearly recognized against the field population. *Right*: With measured star-galaxy classification from ground-based LSST data alone, the main sequence stars of the ultra-faint galaxy is overwhelmed by mis-classified faint unresolved galaxies.

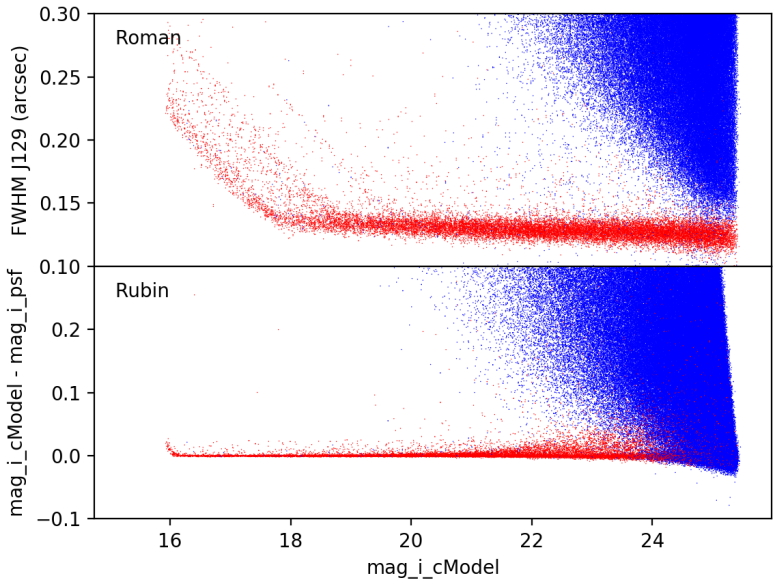

Figure 4: Comparison of star-galaxy classification with Roman and Rubin. Red points correspond to simulated stars and blue points correspond to simulated galaxies. *Top*: Object size (FWHM) measured in Roman J129 band is plotted against LSST i-band flux. *Bottom*: Benchmark object "extendedness" parameter for LSST is plotted against LSST i-band flux. **The space-based angular resolution of Roman enables much more accurate star-galaxy classification at the faint end.**

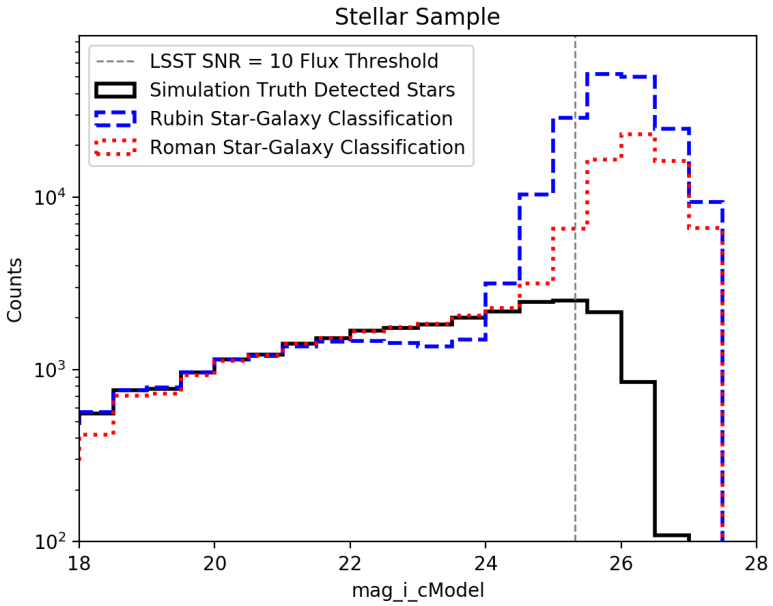

Figure 5: Flux distribution of objects classified as stars based on Rubin (blue) and Roman (red) measurements as compared to the truth simulated flux distribution (black). The sample based on Rubin measurements alone is dominated by mis-classified galaxies fainter than $i \sim 24\,\mathrm{mag}$, and suffers from a loss in completeness at brighter magnitudes. The stellar sample based on Roman measurements in a single band shows better agreement with simulation truth to nearly the SNR=10 depth for LSST.

classification. In addition, the space-based angular resolution of Roman would help to deblend stellar populations at Mpc distances (see Figure 1).

1.2 Extragalactic Stellar Streams

Globular cluster stellar streams in the Milky Way are dynamically cold and can show gap-like features resulting from their interactions with low-mass dark matter subhalos (Yoon et al., 2011; Price-Whelan & Bonaca, 2018; de Boer et al., 2018). This is one of the few known indirect detection methods for low-mass subhalos ($< 10^8$ solar masses), and can help constrain the dark matter subhalo mass functions (e.g., Bullock & Boylan-Kolchin 2017; Bovy et al. 2017; Bonaca et al. 2019). To date, we have only detected globular cluster streams in the Milky Way with a sample size of ≈70 (Shipp et al., 2018; Mateu, 2023). The Rubin Observatory is expected to increase the sample of streams in our Galaxy (Drlica-Wagner et al., 2019). Expanding this population to external galaxies would open up a new era of statistical analyses of gap characteristics in stellar streams, which help distinguish between dark matter models (e.g. fuzzy, warm, cold dark matter).

Pearson et al. (2019) show that Roman will be able to detect GC streams out to $\sim$6 Mpc with a 1 hour exposure. Within this distance, the Rubin footprint includes the luminous galaxies NGC253, Cen A, and M83, as well as many more galaxies in the Sculptor and Cen A groups. Moreover, Aganze et al. (2023) predict the detectability of globular cluster stream gaps with the Roman telescope using resolved stars. They find that gaps from subhalos of masses $\approx 5 \times 10^6$ solar masses in GC streams

hosted in galaxies up to 3 Mpc are detectable with a 1 hour exposure (Z≈28, see Figure 6). This volume contains ≈ 200 galaxies (Karachentsev & Kaisina, 2019), including the galaxies NGC300 and NGC55 in the Rubin footprint (in front of the Sculptor group). While the exposure times quoted here are far beyond the notional HLWAS plans, NGC253, Cen A and most galaxies in the Sculptor and Cen A groups will still be within the GC stream detection limits at HLWAS depth, providing crucial input for deeper GO proposals that could then search for stream gaps (all galaxies mentioned before are reachable for both stellar stream or stream gap discovery when increasing the exposure duration covering the Sculptor and/or Cen A groups to $\sim$500 sec). The feasibility of discovering stellar streams and their gaps depends on density contrasts between the thin but extended stream and the background, requiring a large spatial coverage, a careful Milky Way foreground subtraction and accurate star/galaxy separation. These science goals will therefore strongly benefit from the high resolution and large area that HLWAS can provide. The combination of Rubin proper motions of Milky Way stars and Rubin+Roman colors with Roman resolution will allow improved reduction of contaminant Milky Way foregrounds. Moreover, the WFI instrument slitless spectroscopy of the Roman HLWAS fields will offer validation for the chosen Rubin+Roman color and/or proper motion selections. Simultaneous coverage of Rubin and the WFI Roman fields would therefore enhance the potential for extragalatic stellar stream and stream gap discovery, providing novel constraints on the dark matter subhalo mass function.

2 Considerations for Roman High Latitude Wide Area Survey

Area, Depth, and Location:

The near-field cosmology analyses highlighted in this white paper depend upon **large contiguous sky areas imaged with both Roman and Rubin** because the targets of interest have large angular extent (e.g., Galactic stellar streams) and/or are intrinsically rare (e.g., as-yet-undiscovered ultra-faint galaxies in the Local Volume). The discovery space for such objects scales roughly linearly with the contiguous sky area that can be imaged to a given depth. One particularly exciting science case for Roman + Rubin is the search for a field population of isolated ultra-faint galaxies that would help us to better understand the epoch of reionization and the impact of environment on the formation and growth of the least luminous galaxies. Identifying these field ultra-faint galaxies is uniquely enabled by the combination of wide area, multi-band photometric depth, and accurate star-galaxy classification. We recommend **a high latitude wide area survey with Roman covering a large fraction of the LSST Wide-Fast-Deep footprint in at least one band to a depth such that the faint stars are detected in both surveys.**

The Euclid mission wide survey will provide coverage over most of the LSST footprint ($\sim 15,000$ square degrees) in a wide visible band to a depth of $\sim 26.2\,\mathrm{mag}$ (5σ point source) that is well matched to the LSST depth $i \sim 26.4\,\mathrm{mag}$ (5σ point source) at a similar angular resolution to Roman near-IR imaging (Euclid Collaboration et al., 2022). Guy et al. (2022) describe synergies between Euclid and Rubin as well as several proposed derived data products to enhance studies of resolved stellar populations, including matched catalogs with forced multi-band photometry and joint-pixel star-galaxy classification. With both Rubin and Euclid starting on-sky commissioning in the next year, we will soon be able to directly evaluate the performance of star-galaxy classification and deblending in the combination of the two datasets, and these studies could help to inform the trade between depth and area for the Roman HLWAS to optimize complementarity across the three missions.

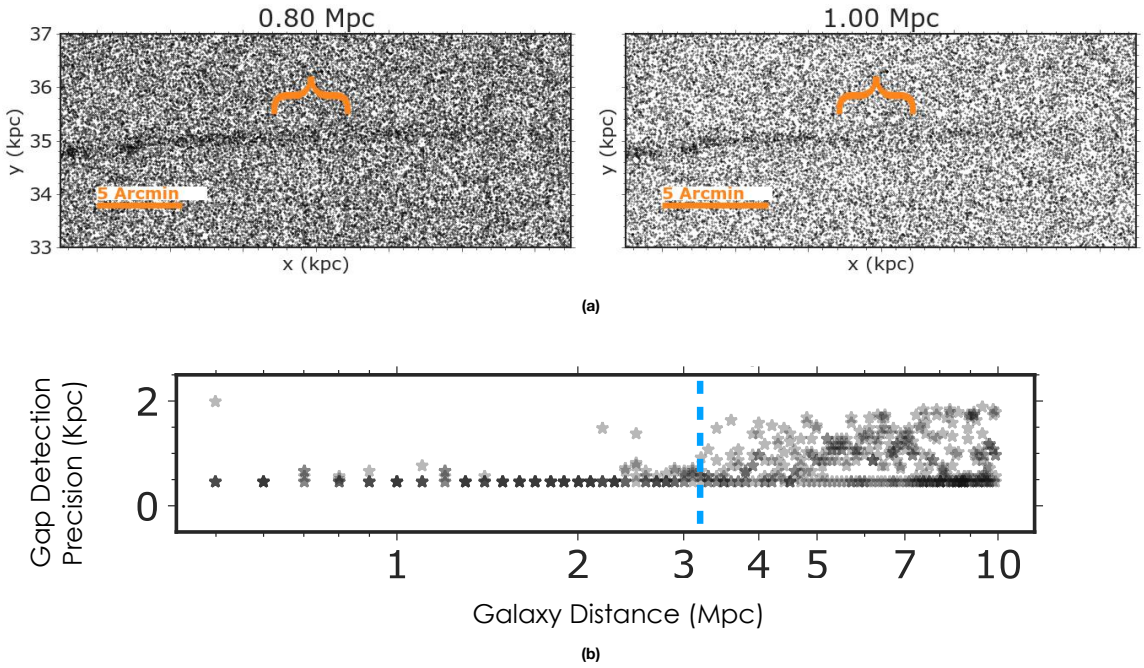

Figure 6: Adapted from Aganze et al. (2023). Top: simulation of a gap in an extragalactic stellar stream, including Milky Way foregrounds at *Roman* magnitude limit of Z≈28 for a host galaxy located at 0.8 Mpc (left) and 1 Mpc (right). Black dots represent resolved stars. Gaps from a subhalo of 5×10^6 solar masses are indicated with the orange brace and the stream is simulated to match the isochrone of Palomar 5 ([Fe/H] = -1.3, Ibata et al. 2017). Bottom: Gap detection precision (in kpc) based on a gap-detection tool developed by Contardo et al. (2022) as a function of distance to the host galaxy. Lower gap detection precision values indicate where the tool is better at localizing the true centers of the gaps. The blue line indicates the detection limit, where the scatter in localizing the gap grows substantially, for a 1-hour exposure.

Filter Coverage:

Based upon the preliminary analyses described in Section 1.1, we expect that the majority of gains in star-galaxy classification accuracy will come from the exquisite angular resolution of Roman (PSF FWHM $\sim 0.26\,\mathrm{arcsec}$). The investigations suggest **similar star-galaxy classification performance for the various Roman filters, and we expect that the wide F146 filter would offer similar performance with increased survey speed**, although F146 photometry was not available in the joint simulated data from Troxel et al. (2023). While stars and galaxies occupy distinct loci in optical-to-near-IR color space, it seems that the photometric uncertainties for faint objects are sufficiently large that this approach is not competitive with morphological classification. Use of color information would be worth exploring further considering the Roman F213 filter, which was not available in the simulation that we analyzed here.

Observing Cadence and Time Baseline:

The star-galaxy separation use case is mostly independent of the detailed implementation of observing cadence and time baseline. To maximize the broad utility of the stellar sample, there would be multiple observing epochs with Roman over a long time baseline to enable proper motion measurements.

Data Management:

Joint pixel processing, or at least forced photometry, would be important to ensure consistent object detection and photometry between the two surveys. We would need robust color measurements to take full advantage of the separation of galaxy and stellar loci in optical + near-IR color space.

Diverse Scientific Opportunities Using a Combined Roman-Rubin Dataset:

While we used cosmic probes of dark matter with ultra-faint galaxies and stellar streams as concrete examples, we emphasize that **nearly all science cases involving faint resolved stellar populations would benefit from coordinated Roman-Rubin observations and analysis**. Furthermore, similar survey concepts to cover much of the LSST Wide-Fast-Deep footprint with a single band of Roman imaging have been considered, e.g., for weak gravitational lensing and galaxy clustering probes of dark energy (Eifler et al., 2021), along with a host of other science cases (Gezari et al., 2022), as described in several related Roman Core Community Survey white papers.

References

Aganze, C., Pearson, S., Starkenburg, T., et al. 2023, arXiv e-prints, arXiv:2305.12045, doi: http://doi.org/10.48550/arXiv.2305.1204510.48550/arXiv.2305.12045

Bonaca, A., Hogg, D. W., Price-Whelan, A. M., & Conroy, C. 2019, , 880, 38, doi: http://doi.org/10.3847/1538-4357/ab287310.3847/1538-4357/ab2873

Bovy, J., Erkal, D., & Sanders, J. L. 2017, , 466, 628, doi: http://doi.org/10.1093/mnras/stw306710.1093/mnras/stw3067

Bullock, J. S., & Boylan-Kolchin, M. 2017, , 55, 343, doi: http://doi.org/10.1146/annurev-astro-091916-05531310.1146/annurev-astro-091916-055313

Contardo, G., Hogg, D. W., Hunt, J. A. S., Peek, J. E. G., & Chen, Y.-C. 2022, , 164, 226, doi: http://doi.org/10.3847/1538-3881/ac961e10.3847/1538-3881/ac961e

de Boer, T. J. L., Belokurov, V., Koposov, S. E., et al. 2018, , 477, 1893, doi: http://doi.org/10.1093/mnras/sty67710.1093/mnras/sty677

Drlica-Wagner, A., Mao, Y.-Y., Adhikari, S., et al. 2019, arXiv e-prints, arXiv:1902.01055, doi: http://doi.org/10.48550/arXiv.1902.0105510.48550/arXiv.1902.01055

Eifler, T., Simet, M., Krause, E., et al. 2021, , 507, 1514, doi: http://doi.org/10.1093/mnras/stab53310.1093/mnras/stab533

Euclid Collaboration, Scaramella, R., Amiaux, J., et al. 2022, , 662, A112, doi: http://doi.org/10.1051/0004-6361/20214193810.1051/0004-6361/202141938

Gezari, S., Bentz, M., De, K., et al. 2022, arXiv e-prints, arXiv:2202.12311, doi: http://doi.org/10.48550/arXiv.2202.1231110.48550/arXiv.2202.12311

Guy, L. P., Cuillandre, J.-C., Bachelet, E., et al. 2022, in Zenodo id. 5836022, Vol. 58, 5836022, doi: http://doi.org/10.5281/zenodo.583602210.5281/zenodo.5836022

Ibata, R. A., Lewis, G. F., Thomas, G., Martin, N. F., & Chapman, S. 2017, , 842, 120, doi: http://doi.org/10.3847/1538-4357/aa751410.3847/1538-4357/aa7514

Karachentsev, I. D., & Kaisina, E. I. 2019, Astrophysical Bulletin, 74, 111, doi: http://doi.org/10.1134/S199034131902001910.1134/S1990341319020019

Mateu, C. 2023, , 520, 5225, doi: http://doi.org/10.1093/mnras/stad32110.1093/mnras/stad321

Mutlu-Pakdil, B., Sand, D. J., Crnojević, D., et al. 2021, , 918, 88, doi: http://doi.org/10.3847/1538-4357/ac0db810.3847/1538-4357/ac0db8

Nadler, E. O., Drlica-Wagner, A., Bechtol, K., et al. 2021, , 126, 091101, doi: http://doi.org/10.1103/PhysRevLett.126.09110110.1103/PhysRevLett.126.091101

Pearson, S., Starkenburg, T. K., Johnston, K. V., et al. 2019, , 883, 87, doi: http://doi.org/10.3847/1538-4357/ab3e0610.3847/1538-4357/ab3e06

Price-Whelan, A. M., & Bonaca, A. 2018, , 863, L20, doi: http://doi.org/10.3847/2041-8213/aad7b510.3847/2041-8213/aad7b5

Shipp, N., Drlica-Wagner, A., Balbinot, E., et al. 2018, , 862, 114, doi: http://doi.org/10.3847/1538-4357/aacdab10.3847/1538-4357/aacdab

Troxel, M. A., Lin, C., Park, A., et al. 2023, , 522, 2801, doi: http://doi.org/10.1093/mnras/stad66410.1093/mnras/stad664

Yoon, J. H., Johnston, K. V., & Hogg, D. W. 2011, , 731, 58, doi: http://doi.org/10.1088/0004-637X/731/1/5810.1088/0004-637X/731/1/58